LAWRENCE
LIVERMORE
NATIONAL
LABORATORY

LLNL-PROC-403056

Geomechanical Simulations of Caprock Integrity Using the Livermore Distinict Element Method

J. Morris, S. Johnson, S. J. Friedmann

April 22, 2008

Seventh Annual Conference on Carbon Capture and Sequestration
Pittsburgh, PA, United States
May 5, 2008 through May 8, 2008

CONFERENCE PROCEEDINGS

Geomechanical Simulations of Caprock Integrity Using the Livermore Distinict Element Method

Joseph P. Morris, Atmospheric, Earth and Energy Division, Mail Code L-206, Lawrence Livermore National Laboratory, 7200 East St., Livermore, CA 94550, Phone: 925-424-4581, e-mail morris50@llnl.gov

Scott M. Johnson, Atmospheric, Earth and Energy Division, Mail Code L-206, Lawrence Livermore National Laboratory, 7200 East St., Livermore, CA 94550, Phone: 925-424-6246, e-mail johnson346@llnl.gov

Samuel J. Friedmann, Global Security, Mail Code L-175, Lawrence Livermore National Laboratory, 7200 East St., Livermore, CA 94550, Phone: 925-423-0585, e-mail friedmann2@llnl.gov

SEVENTH ANNUAL CONFERENCE ON CARBON CAPTURE AND SEQUESTRATION - DOE/NETL
May 5 – 8, 2008

Abstract

Large-scale carbon capture and sequestration (CCS) projects involving annual injections of millions of tons of CO2 are a key infrastructural element needed to substantially reduce greenhouse gas emissions. The large rate and volume of injection will induce pressure and stress gradients within the formation that could activate existing fractures and faults, or drive new fractures through the caprock. We will present results of an ongoing investigation to identify conditions that will activate existing fractures/faults or make new fractures within the caprock using the Livermore Distinct Element Code (LDEC). LDEC is a multiphysics code, developed at LLNL, capable of simulating dynamic fracture of rock masses under a range of conditions. As part of a recent project, LDEC has been extended to consider fault activation and dynamic fracture of rock masses due to pressurization of the pore-space. We will present several demonstrations of LDEC functionality and an application of LDEC to a CO2 injection scenario.

We present results from our investigations of Teapot Dome using LDEC to study the potential for fault activation during injection. Using this approach, we built finite element models of the rock masses surrounding bounding faults and explicitly simulated the compression and shear on the fault interface. A CO2 injection source was introduced and the area of fault activation was predicted as a function of injection rate. This work presents an approach where the interactions of all locations on the fault are considered in response to specific injection scenarios. For example, with LDEC, as regions of the fault fail, the shear load is taken up elsewhere on the fault. The results of this study are consistent with previous studies of Teapot Dome and indicate significantly elevated pore pressures are required to activate the bounding faults, given the assumed in situ stress state on the faults.

Introduction

Large scale carbon capture and sequestration (CCS) raises many diverse geomechanical challenges. A successful CCS scenario typically involves injection of millions of tons of CO2 per year into a porous, permeable formation overlaid with an impermeable caprock. However the storage integrity could fail due to activation of preexisting faults or creation of new fractures in the caprock. These potential failure modes involve combinations of both continuum and discrete processes. This work discusses recent extensions to the Livermore Distinct Element Code (LDEC), a fully-coupled fluid-flow discrete/finite element simulation code, that are being used to evaluate the geomechanical sources of risk to successful CCS.

LDEC was originally developed by Morris et al. (2002) as a distinct element (DEM) code to simulate the response of jointed geologic media to dynamic loading. Cundall and Hart (1992) review a number of numerical techniques that have been developed to simulate the behavior of discontinuous systems using DEMs. The DEM is naturally suited to simulating such systems because it can explicitly accommodate the blocky nature of natural rock masses. For example, Figure 1 shows a jointed medium, typical of the early applications of LDEC. LDEC was later extended to include Finite Element-Discrete Element transition (Morris et al, 2006), including an extension to include a nodal cohesive element formulation, which allows the study of fracture problems in the continuum-discontinuum setting with reduced mesh dependence (Block et al., 2007). Additionally, LDEC supports fully-coupled fluid flow using both Smooth Particle Hydrodynamics (SPH) and unstructured fracture flow mesh methods.

This paper describes the continuum and discrete mechanics capabilities currently implemented in LDEC and presents several applications of LDEC. Finally, we document the application of LDEC to predicting potential fault activation during CCS.

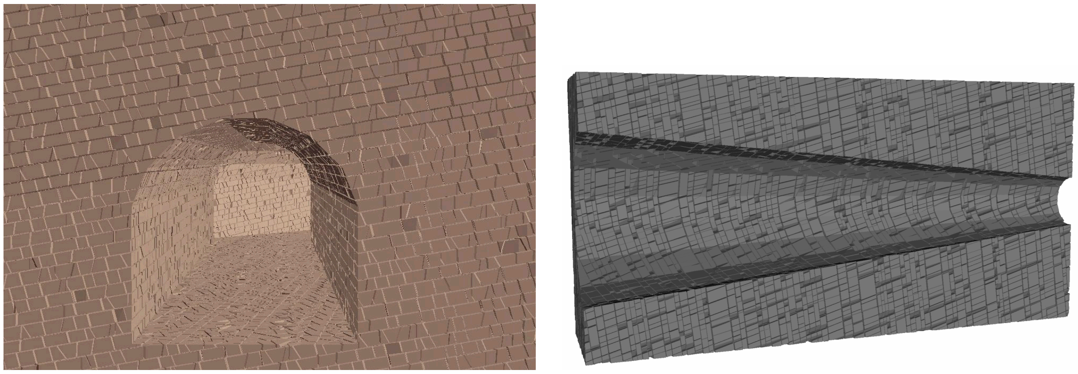

Figure 1: Two examples of LDEC geomechanical computational domains. A tunnel in jointed rock and a cavity in coal. Both models include non-persistent and randomized joint sets. LDEC was designed to calculate the evolving mechanical properties of such structures as they fail under different loading conditions.

Treatment of Geologic Media Using LDEC

In the simplest case, the Livermore Distinct Element Code can be run in a rigid-block mode, so that all deformation in the system is captured in the behavior of the contacts. The most complicated aspect of the code is then related to contact detection. In general, the equations of motion of the elements are determined in a standard manner by integrating vector equations for both the center of mass of each element and an orthonormal vector triad that determines its absolute orientation. Contact detection monitors how the connectivity changes as a result of relative block motion. The Lagrangian nature of the DEM also simplifies tracking of material properties as blocks move, and it is possible to guarantee exact conservation of linear and angular momentum throughout the computation. This rigid block mode permits efficient solution extensively jointed, hard rock masses.

LDEC also supports deformation within the intact rock blocks. In Morris et al. (2004), it was observed that the theory of a Cosserat point (2000) can model each element as a homogenously deformable continuum. A Cosserat point describes the dynamic response of the polyhedral rock block by enforcing a balance of linear momentum to determine the motion of the center of mass, as well as three vector balance laws of director momentum to determine a triad of deformable vectors, which model both the orientation of the element and its deformation. The response of the deformable polyhedral block is modeled explicitly using the standard nonlinear constitutive equations that characterize the original three-dimensional material. This approach introduces a form of deformability into the arbitrary polyhedral blocks without the computational overhead of finite elements. See Morris et al. (2004) for applications of this mode of LDEC.

To address problems where single homogeneously deformable elements are inappropriate the arbitrary polyhedral blocks can be sub-discretized into a tetrahedral Cosserat mesh. The numerical solution procedure depends on nodal balance laws to determine the motion of the four nodes of each tetrahedral element, similar to that described above for the motion of blocks. In continuum regions, where the nodes of neighboring elements remain common (i.e., unbreakable), the Cosserat point formulation is basically the same as standard finite element models (FEM) that use homogeneously deformable tetrahedral elements. However, the shared nodes linking the elements can be dynamically split in response to user specified criteria. LDEC can be run simultaneously in DEM and FEM-like modes, dynamically blending continuum and discrete regions, as necessary and new contact surfaces are automatically created within the rock as they are created. For example, Block et al. (2007) applied LDEC to the simulation of crack branching in a plate under tensile stress (see Figure 2).

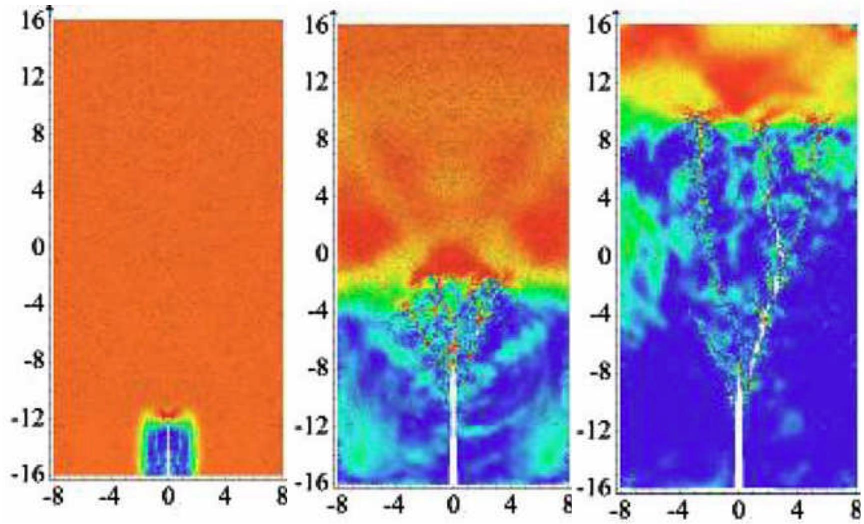

Figure 2: Maximum principal stress for branching at 1, 15, and 30μs after initial of a loaded cracked plate using LDEC. Blue indicates zero stress and red indicates 100% of the tensile strength. See Block et al (2007) for details.

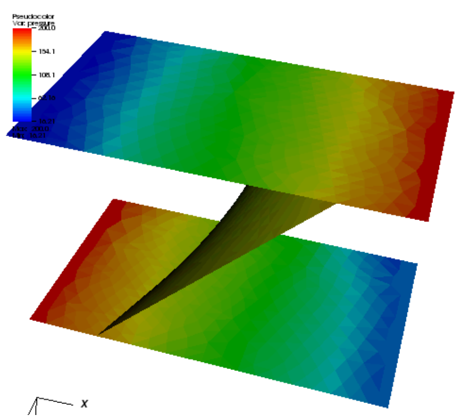

Figure 3: Example of an unstructured fracture flow network simulated using LDEC. This flow network (consisting of triangular elements) is coupled to the mechanical deformation of the surrounding tetrahedral finite elements.

Treatment of Fluid Flow in LDEC

LDEC supports fully coupled fluid flow by two different mechanisms: Smooth Particle Hydrodynamics (see Monaghan, 1992, for a review) and a finite difference unstructured mesh. The SPH approach is most appropriate for fluid-solid interaction where the fluid occupies a three-dimensional volume. However, fluid driven fracture involves fluid motion in a highly confined geometry which is not amenable to fully-3D solution. For this reason, we have implemented a finite difference. LDEC also supports coupled fluid flow using unstructured triangular elements similar to that presented by CITATION. In contrast with CITATION, the LDEC fracture network can extend in response to mechanical damage. At the time of writing, this capability has only recently been incorporated into LDEC and is yet to be applied to fluid driven fracture simulation. In contrast, the following section presents an application of LDEC to CO_2 which considers activation of a pre-existing fault due to elevated pore pressure.

Application of LDEC to Fault Activation during CO2 Sequestration

We will now present initial results from our ongoing study where LDEC is being utilized to directly simulate scenarios relevant to CO_2 sequestration. This initial work was focussed upon potential scenarios related to CO_2 injection at Teapot Dome. Chiaramonte et al. (2007) describe Teapot Dome in detail, including estimates of the in situ stress and the geometry of the bounding caprock and faults. In particular, Chiaramonte et al. (2007) identified a specific bounding fault (designated S1) as representing a risk to containment of the CO_2. Using an approach similar to that of Chiaramonte et al. (2007) we considered the projection of the measured in situ stress field onto a detailed discretization of the S1 fault and calculated the pore pressure increase that would result in slip at any location of the fault (see Figure 4).

The second phase of our study of Teapot Dome used LDEC to study the potential for fault activation during injection. Using this approach, we built tetrahedral finite element models of the rock masses surrounding the S1 fault and explicitly simulated the compression and shear on the fault interface. LDEC automatically detects where the tetrahedral elements of the opposing fault surfaces make contact and generates “contact elements”. It is these individual contact elements that carry the normal and shear load across the fault. A Coulomb friction law was assumed on each contact with a coefficient of friction of 0.6. An effective stress rule was assumed such that the shear strength on the fault depends upon the normal stress at that location minus the pore pressure. Thus, when the CO2 injection source was introduced and the pore-pressure is increased, the effective stress on the fault lowers and we can predict the area of fault activation as a function of injection rate. In the past, LDEC has imported pore pressure histories from external codes, such as NUFT (Johnson et al., 2004). For this case study, an analytic pore pressure distribution was introduced by assuming a point source injection in an infinite medium. This analysis may be contrasted with the analysis shown in Figure 4 which analyzed the fault surface at discrete locations and identified the level of elevated pore pressure required to activate a given location on the fault in isolation. The LDEC simulation models the interactions of all locations on the fault in response to specific injection scenarios. For example, with LDEC, as regions of the fault fail, the shear load is supported elsewhere on the fault, leading to progressive failure of the fault.

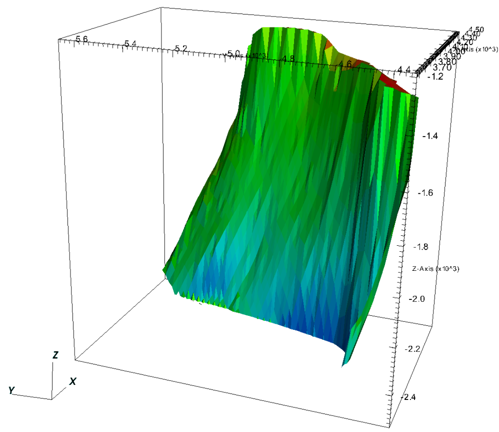

Figure 4: Prediction of pore pressure increase required to activate the S1-fault using an approach similar to Chiaramonte et al. (2007). Blue corresponds to an increase of 35 MPa pore pressure to activate the fault.

Deleted: increase

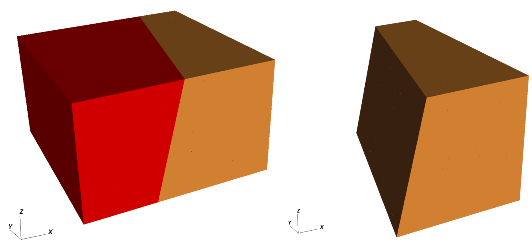

Figure 5: LDEC geometry of the S1 fault region. The domain spanned a depth of 1200m through 2400m. The coordinate system has the x-axis aligned with the Sig_Hmax direction, y-axis is aligned with the Sig_Hmin direction and z-axis is vertical.

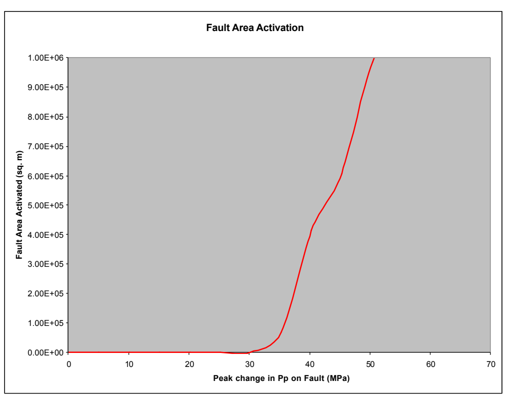

Figure 6: Plot of area of fault that has slipped as a function of the elevation in pore pressure at the location on the fault closest to the injection point (a depth of ~1800m). The fault starts to activate when the pore pressure is elevated by approximately 30MPa at this location. The fault area activated rapidly grows with increasing pore pressure as load is transferred to neighboring locations on the fault.

For simplicity, the LDEC simulation considered a single planar fault (see Figure 4). The domain spanned a depth of 1200m through 2400m and the boundary conditions reproduced the in-situ stress state documented by Chiaramonte et al. (2007). The specific case considered corresponds to point injection at a depth of 1800m, approximately 160m laterally away from the fault. Figure 5 shows the area of fault activated in the simulation as a function of elevation in pore pressure at the location on the fault closest to the injection point. The fault starts to activate when the pore pressure is elevated by approximately 30MPa at the location on the fault closest to the injection point. The fault area activated rapidly grows with increasing pore pressure as load is transferred to neighboring locations on the fault. The results of this study are consistent with Chiaramonte et al. (2007). Specifically, given the reported in situ stress state on the fault significantly elevated pore pressure is required to activate the S1 fault.

Conclusions

The Livermore Distinct Element Code (LDEC) has been used to study a wide variety of problems in geomechanical fracture and fragmentation, including dynamic and quasi-static analysis of fluid-initiated fracture and fault activation. The current version of LDEC provides simultaneous DEM and FEM-like domain partitioning, as well as the possibility of converting between the two modes dynamically. We have extended LDEC to include features relevant to simulation of fault activation due to CO2 injection and were able to obtain results consistent with a previous case study that employed entirely different tools.
Future work will include applying LDEC to additional site specific CO2 injection case studies. We are currently enhancing the LDEC treatment of pore pressure to include a wider range of injection scenarios. In addition, LDEC is now coupled to a dynamic fracture flow capability to support simulation of fluid driven fracturing events within a fracture network. This latter capability will be used to establish what combination of parameters may result in mechanical damage to the caprock due to hydraulic fracturing events.

Acknowledgements

This work performed under the auspices of the U.S. Department of Energy by Lawrence Livermore National Laboratory under Contract DE-AC52-07NA27344.

References

Block, G., Rubin, M.B., Morris, J., Berryman, J.G., Simulations of dynamic crack propagation in brittle materials using nodal cohesive forces and continuum damage mechanics in the dinstinct element code LDEC, International Journal of Fracture, 144:131-147, 2007.

Cundall, P. A. and Hart, D. H., Numerical modeling of discontinua, Eng. Comput., 9, 1992, 101-113

Chiaramonte, L., M. D. Zoback, J. Friedman, V. Stamp, “Seal integrity and feasibility of CO2 sequestration in the Teapot Dome EOR pilot: geomechanical site characterization,” Environ. Geol., 2007.

Johnson, J.W., Nitao, J.J., Morris, J.P., (2004), “Reactive transport modeling of cap rock integrity during natural and engineered CO2 storage,” in S. Benson (ed.), CO2 Capture Project Summary Volume (2), Elsevier.

Monaghan, J. J., Smoothed Particle Hydrodynamics, Annual Reviews in Astronomy and Astrophysics, 30, 1992, 543-574

Morris, J. P., Glenn, L. A., and Blair, S. C., The distinct element method - application to structures in jointed rock, in Lecture Notes in Computational Science and Engineering: Meshfree Methods, 26, Springer-Verlag, Heidelberg, 2002, pp. 291-306.

Morris, J. P., Rubin, M. B., Blair, S. C., Glenn, L. A., and Heuze, F. E., Simulations of underground structures subjected to dynamic loading using the distinct element method, Engng Comput., 21, 2004, 384-408.

Morris, J. P., Rubin, M. B., Block, G. I., Bonner, M.P., Simulations of Fracture and Fragmentation of Geologic Materials using Combined FEM/DEM Analysis, International Journal of Impact Engineering, 33, 2006, 463-473

Morris, J.P., Fox, P.J., and Zhu, Y., Modeling low Reynolds number flows using SPH, J. Comput. Phys. 136, 1997, 214-226

Morris, J. P., Simulating surface tension with Smoothed Particle Hydrodynamics, Int. J. Numer. Meth. Fluid Flow, 33, 2000, 333-353.

Rubin, M. B. Cosserat Theories: Shells, Rods and Points, Solid Mechanics and its Applications, Kluwer, The Netherlands, 2000.